Erschienen in: Journal of the American Chemical Society. ACS Publications. 2024, 146(24), S. 16590-16600
https://doi.org/10.1021/jacs.4c03498

Thermostable WW-Domain Scaffold to Design Functional β-Sheet Miniproteins

Christina Lindner, Anke Friemel, Niklas Schwegler, Lisa Timmermann, Truc Lam Pham, Vanessa Reusche, Michael Kovermann,* and Franziska Thomas*

ABSTRACT: There has been a recent surge in the design of miniproteins for medicinal chemistry, biomaterial design, or synthetic biology. In particular, there is an interest in peptide scaffolds that fold reliably, predictably, and with solid stability. In this article, we present the design of a highly thermostable WW domain, a three-stranded β-sheet motif, with a superior melting temperature of about 90 °C to serve as a core scaffold onto which receptor-like properties can be grafted. We have performed specific rounds of sequence iteration on a WW-domain consensus sequence to decipher sequence positions that affect structural and, thus, thermal stability. We identified a sequence−structure relationship that yields a highly thermostable WW-domain scaffold. High-resolution NMR spectroscopy was applied, which enabled the identification of structural features at the atomic scale that contribute to this high thermostability. Finally, we grafted the binding motifs of the three WW-domain groups—Group I, Group II/III, and Group IV—and organophosphate and metal binding onto the highly thermostable WW-domain scaffold and obtained thermostable *de novo* WW domains that indeed display the different binding modes that were intended. The organophosphate-binding WW domains exhibit melting temperatures that are up to 34 K higher than previously reported top-down designs. These results impressively demonstrate that the highly thermostable WW-domain core scaffold is a solid platform for the design of discrete and reliably folding functional β-sheet peptide miniproteins, providing an essential addition to the toolbox of peptide scaffolds previously used in synthetic biology and material design.

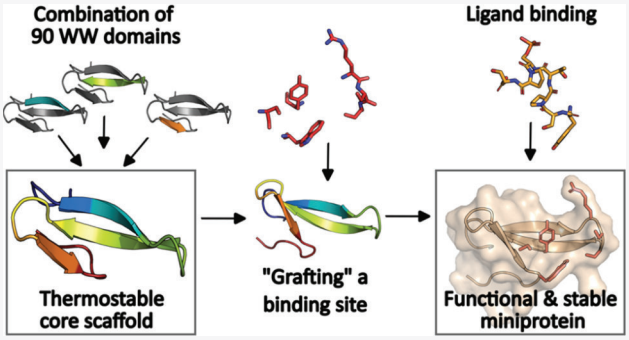

INTRODUCTION

Miniproteins, folded peptides <100 amino acids, are promising scaffolds for applications in synthetic biology and biomaterial design,[1] but also in medicinal chemistry, particularly in the development of new peptide therapeutics, *e.g.*, to target protein−protein interactions.[2] The appeal of miniproteins lies in their reduced complexity, which allows us to improve our understanding of sequence−structure−stability and sequence−structure−function relationships in proteins in general but also to provide well-defined peptide scaffolds on which function can ideally be engineered in a highly predictable manner.[1]

The sequence−structure relationships of most miniproteins are only partially understood, if at all. Most design activities therefore rely on miniproteins from natural sources that have been engineered top-down to alter their function.[1] This approach has a major drawback: mutations to change the function of an evolutionarily optimized biologically active protein are often structurally destabilizing, commonly referred to as stability−function trade-off.[3] This does not mean that the new function cannot be designed as desired, but the modified scaffold often lacks the thermostability required to be used reliably for the intended application. Interestingly, every folded protein scaffold has a so-called threshold robustness, a margin of thermal stability that can be exploited before a protein loses its fitness.[3] This threshold robustness is greater for highly thermostable proteins, *i.e.*, proteins that are functional above 60 °C.[4] As this also applies to miniproteins, it is important to invest research activities in the development of thermally and thus structurally stable miniprotein scaffolds that fold reliably and predictably and from which thermostable functional miniproteins with a predictable structure can be obtained, *e.g.*, for *in vivo* applications.[5]

One class of miniproteins that has been shown to be readily functionalized is that of WW domains, three-stranded, antiparallel β-sheet peptides of approximately 35 amino acids that bind to proline-rich peptide sequences.[6] The WW-domain

scaffold accepts drastic sequential changes such as loop modification and circular permutation.[7] There are also, albeit few, examples of native WW domains that have been engineered to exhibit alternative function,[6f] *e.g.*, binding to single-stranded DNA or metal ion and organophosphate binding.[7d,8] However, some of these functional scaffolds display low melting temperatures of approximately 35 °C.[7d,8b] Recently, the zinc-binding WW domain was redesigned to optimize its thermal stability, which in turn led to improved function, demonstrating the importance of considering both function and stability in peptide design.[8d]

In order to establish the WW-domain scaffold in the field of functional miniprotein design, it is essential to gain a comprehensive knowledge of the sequence−structure−function relationships that will allow us to design scaffolds with excellent thermal stability, which can then be used as a platform to generate thermostable functional miniproteins. There are studies that partially address one or the other aspect: *e.g.*, highly thermostable WW domains have been described, but structure-stabilizing measures were bespoke, and/or thermostability was achieved at the expense of function.[7b,c] Mutagenesis studies have also been carried out, but these have not led to the development of a thermostable WW-domain scaffold.[6a] Even *de novo* design of WW domains has been achieved, but again without the intention of providing thermostable scaffolds.[9]

Herein, we present the design of highly thermostable WW-domain scaffolds to be used as engineering platforms to generate functional WW-domain-based miniproteins. We performed iterative modification of a WW-domain consensus sequence (Figure 1a,b). Based on these results, we were able to formulate rules for designing thermostable WW-domain scaffolds with melting temperatures of approximately 90 °C and higher (Figure 1c). Using multidimensional NMR spectroscopy, we have also determined the highly resolved three-dimensional structure of such a highly stable WW domain. The thermostable WW domains found here are intended to be core scaffolds that can be functionalized by simply grafting a binding site of choice onto their surface (Figure 1d). To prove this concept, we have successfully designed Group I, II/III, and IV WW domains as well as WW domains with organophosphate and metal ion binding properties. All functional WW-domain minireceptors exhibit good to excellent thermal stability, with one phosphocholine minireceptor having a melting temperature approximately 34 K higher than the corresponding functional variant obtained by top-down design,[7d] highlighting the importance of this study.

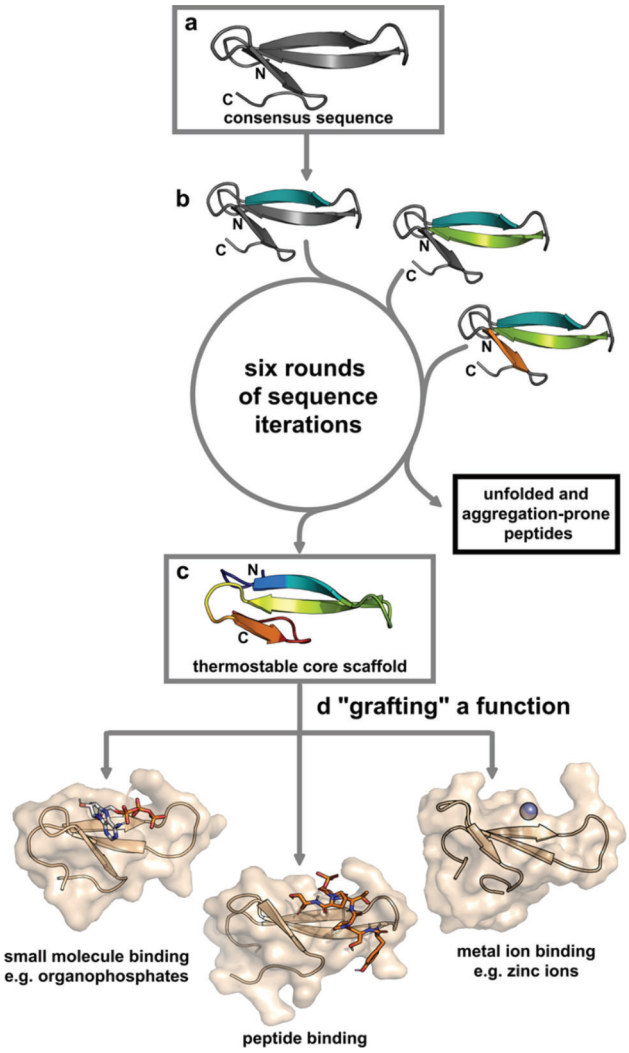

Figure 1. Iterative design approach to obtain a highly thermostable WW-domain scaffold. The design approach consists of the following steps: (a) generation of a consensus sequence; (b) six rounds of sequence iterations from the N- to the C-terminus and selection for thermal stability and structural integrity (exemplarily, the first three rounds of iterations are shown); (c) design of a highly thermostable WW-domain core scaffold; and (d) grafting of functional sites onto the core scaffold.

RESULTS AND DISCUSSION

WW-Domain Consensus Sequence. As a starting point for our rational design of a WW-domain core scaffold, we generated a consensus sequence WW-CS (CS−consensus, Figure 1a) serving as a solid reference (Figure 2a,b and Table S1).[9b,c] At most positions in the consensus sequence, we chose the amino acid residue with the highest statistical abundance. However, to avoid aspartimide formation in chemical synthesis, we omitted aspartate where possible. Only in sequence position 11, we felt this was not an option, as there was a possibility that this aspartate might be involved in electrostatic interactions. WW-CS was synthesized by microwave-assisted solid-phase peptide synthesis. Secondary structure and thermal stability were then studied by circular dichroism (CD) spectroscopy (Figure 2c,d). The corresponding CD spectrum of WW-CS with the characteristic maximum at 228 nm and a minimum at 215 nm, which results from the exciton coupling between W6 and Y19 and the three-stranded β-sheet structure, shows the typical CD spectroscopic pattern of a WW domain. The thermal stability of WW-CS was elucidated by monitoring the CD signal at 228 nm, dependent on temperature. The resulting sigmoidal thermal denaturation profile showed a cooperative transition from a properly folded to a rather unstructured polypeptide, and a two-state folding model was then used for the fitting procedure (see Supporting Information (SI), eq 3).[10] This resulted in a melting temperature of T_m = 53.5 °C for thermal denaturation of WW-CS.

Iterative Approach to Explore the Sequence−Structure Relationship. Starting from WW-CS, we followed an iterative approach to experimentally identify residues that are relevant to the structural integrity of the WW domain and

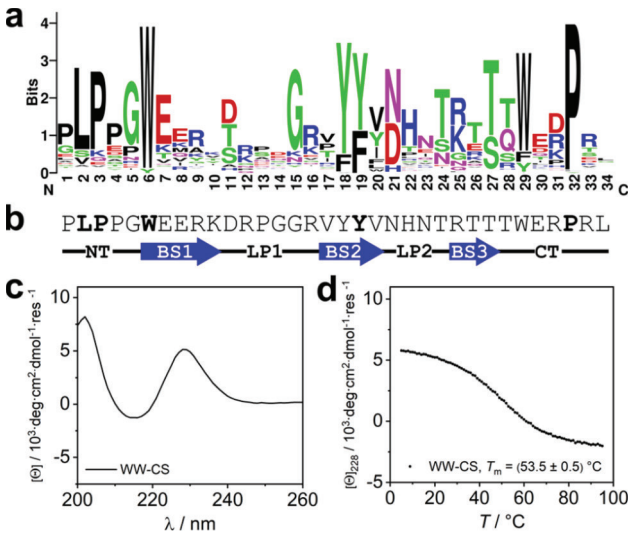

Figure 2. WW-domain consensus sequence. (a) WebLogo (http://weblogo.berkeley.edu/)[11] generated from a sequence alignment of 90 WW domains (Table S1; see the SI for more details). (b) WW-domain consensus sequence WW-CS (residues in bold form the hydrophobic core of the WW domain or are otherwise highly conserved) and schematic representation of β-sheet (BS, blue arrow), loop/disordered regions (LP, black line), and the N- and C-terminus (NT, CT, black line). (c) CD spectrum of WW-CS at T = 20 °C; (d) thermal denaturation profile of WW-CS monitored at 228 nm leading to a transition midpoint of T_m = 53.5 °C (0.1 mM peptide, phosphate-buffered saline (PBS), pH 7.5).

that may enhance thermal stability (Figure 1b). The scaffold of the WW domain comprises three β-strands referred to as BS1, BS2, and BS3, going from the N- to the C-terminus (CT), including two loops (LP1 and LP2). We consecutively varied the sequences of each structural element (BS1, LP1, BS2, LP2, BS3, CT) and carried over the best hit in terms of structural integrity and thermal stability to the next round of iterations (Table 1). The N-terminal segment (NT, residues 1−5) was not modified, as it displays a high degree of conservation. A slightly modified consensus sequence was used as input for the iterative rounds of sequence modification. We chose an alternating pattern of hydrophobic (h) and polar (p) residues (hphph) in the strand regions (BS1: Wphph, BS2: IYFY, BS3: pTp), the classical design scheme for amphipathic β-sheet peptides, with special consideration of β-branched amino acids (isoleucine and threonine) and aromatic amino acids, as they have high β-sheet propensity.[12] We assumed that the extension of the hydrophobic core by using additional hydrophobic residues should increase the thermal stability of the WW-domain scaffold. We also aimed to keep the loop sequences as simple as possible; hence, we chose sequences rich in flexible serine and glycine residues that have been commonly used for loop regions in designed peptides.[13]

We have deliberately iterated from the N- to the C-terminus (probing 37 variants in total) as this direction is reasonable in view of LP1 having been described as the initial nucleation site for folding.[14] In addition, we considered a study by the Kelly group, which performed extensive alanine and glycine scans in the WW domain of hPin1 ($hPin1_{WW}$) to investigate the relevance of specific residues for the thermal stability of this specific WW domain.[6a] We used CD spectroscopy and CD spectroscopic thermal denaturation experiments to evaluate the structure and thermal stabilities of the peptides obtained by this sequence iteration (Figures S1−S2 and Table 1).

In the following, only a brief summary of the main results of the sequence iterations is given. For a detailed description, see the Supporting Information (Chapter 2.1). For the BS1 segment (residues 6−10) with the general sequence pattern Wphph, we found that isoleucine was most stabilizing at both hydrophobic positions due to its high β-propensity,[12b] as was the presence of oppositely charged residues at polar sequence positions 7 and 9. WW-BS1−1—containing a WEIRI motif—showed the highest thermal stability, with a melting temperature of 16 K higher than the consensus sequence (Table 1, entry 2 and Figure S2a).

The sequence segment LP1 (residues 11−16) does not display a high degree of conservation, except for glycine at position 15 and oppositely charged residues at positions 11 and 16. The conserved glycine residue is indeed essential for the structural integrity. WW-domain variants with different residues at this position tend to aggregate over time (Table 1, entries 9−12). Oppositely charged residues at positions 11 and 16 lead to a high degree of structural stabilization (Table 1, entries 14−15 and Figures S1b and S2b), yielding WW domains with T_m values of 85.0 and 79.5 °C, respectively. Since LP1 is crucial for the folding of the WW domain, we propose that these residues stabilize β-hairpin formation through electrostatic interactions.

BS2 (residues 17−20) preferentially contains aromatic amino acids (Figure 2a). The best structural stabilization is achieved when tyrosine is positioned in the hydrophobic core (position 19) (Table 1, entry 16 and Figure S2c). Phenylalanine at this position (WW-LP1−5) leads to a properly folded WW domain but with lower thermal stability (Figures S1c and S2c). The WW-BS2−1 variant with the IYYY motif was best in terms of structure and thermal stability.

LP2 (residues 21−24) has been shown to be less tolerant of sequence variation than LP1. While asparagine 21 at the beginning of LP2 is highly conserved (Figure 2a), we found that either serine or threonine are required at the end of the loop (Table 1 and Figures S1d and S2d). Incorporating glycine at this position resulted in an unfolded structural pattern (Table 1, entries 26−27 and Figure S1d). Hydrophobic amino acids at position 23 led to WW-domain variants with increased thermal stability (Table 1, entries 24, 25, 28 and Figure S2d). The LP2 variant possessing the highest thermal stability is WW-LP2−5 with an NSIT sequence motif.

BS3 (residues 25−27) prefers a positively charged amino acid at position 25 and serine or threonine residues at the other two positions (Figure 2a). Lysine or arginine have indeed been shown to be interchangeable (Table 1). When threonine at position 26 is replaced by a nonpolar β-branched amino acid (Table 1, entry 35), the peptide tends to aggregate. Threonine at position 27 gives the WW-BS3 variant with the highest thermal stability (Table 1, entry 32 and Figures S1e and S2e), but other polar amino acids such as serine and asparagine or nonpolar alanine are also tolerated.

We have finalized our step-by-step approach of sequence iterations with the investigation of the C-terminal segment. We could confirm the previously reported mutability of W29, since substitution with alanine led to only a marginal loss of thermostability while maintaining a stable WW-domain structure (Table 1, entry 36 and Figures S1f and S2f). On sequence position 30, hydrogen bond acceptors are required (Table 1 entry 37).[15] Shortening the C-terminus by two amino

Table 1. Sequences and Melting Temperatures of Peptides Derived from Sequence Iterations of WW-CS

Iteration	entry	WW domain	Sequence ---NT------BS1-------LP1------BS2—-LP2---BS3-------CT--- 1---------10----------20----------30---	T_m / °C
	1	WW-CS	Ac-PLPPG-WEERK-DRPGGR-VYYV-NHNT-RTT-TWERPRL-NH_2	53.5 ± 0.5
1	2	WW-BS1-1	Ac-PLPPG-**WEIRI**-DRPGGR-IYFY-NHNT-KTT-TWERPRL-NH_2	69.5 ± 0.5
	3	WW-BS1-2	Ac-PLPPG-**WEIRL**-DRPGGR-IYFY-NHNT-KTT-TWERPRL-NH_2	66.0 ± 0.5
	4	WW-BS1-3	Ac-PLPPG-**WEIRT**-DRPGGR-IYFY-NHNT-KTT-TWERPRL-NH_2	65.5 ± 0.5
	5	WW-BS1-4	Ac-PLPPG-**WEIKI**-DRPGGR-IYFY-NHNT-KTT-TWERPRL-NH_2	65.5 ± 0.5
	6	WW-BS1-5	Ac-PLPPG-**WEIEI**-DRPGGR-IYFY-NHNT-KTT-TWERPRL-NH_2	24.5 ± 1.0
	7	WW-BS1-6	Ac-PLPPG-**WKIKI**-DRPGGR-IYFY-NHNT-KTT-TWERPRL-NH_2	49.5 ± 0.5
	8	WW-BS1-7	Ac-PLPPG-**WQIQI**-DRPGGR-IYFY-NHNT-KTT-TWERPRL-NH_2	51.0 ± 0.5
2	9	WW-LP1-1[a]	Ac-PLPPG-WEIRI-**SGSGSG**-IYFY-NHNT-KTT-TWERPRL-NH_2	51.5 ± 0.5
	10	WW-LP1-2[a]	Ac-PLPPG-WEIRI-**DGSGSK**-IYFY-NHNT-KTT-TWERPRL-NH_2	60.5 ± 0.5
	11	WW-LP1-3[a]	Ac-PLPPG-WEIRI-**DGSGSR**-IYFY-NHNT-KTT-TWERPRL-NH_2	62.5 ± 0.5
	12	WW-LP1-4[a]	Ac-PLPPG-WEIRI-**EGSGSR**-IYFY-NHNT-KTT-TWERPRL-NH_2	57.5 ± 0.5
	13	WW-LP1-5	Ac-PLPPG-WEIRI-**GSGSGS**-IYFY-NHNT-KTT-TWERPRL-NH_2	53.5 ± 0.5
	14	WW-LP1-6	Ac-PLPPG-WEIRI-**DSGSGR**-IYFY-NHNT-KTT-TWERPRL-NH_2	85.0 ± 0.5
	15	WW-LP1-7	Ac-PLPPG-WEIRI-**ESGSGR**-IYFY-NHNT-KTT-TWERPRL-NH_2	79.5 ± 0.5
3	16	WW-BS2-1	Ac-PLPPG-WEIRI-GSGSGS-**IYYY**-NHNT-KTT-TWERPRL-NH_2	58.0 ± 0.5
	17	WW-BS2-2	Ac-PLPPG-WEIRI-GSGSGS-**ISYY**-NHNT-KTT-TWERPRL-NH_2	46.5 ± 0.5
	18	WW-BS2-3	Ac-PLPPG-WEIRI-GSGSGS-**IFFY**-NHNT-KTT-TWERPRL-NH_2	51.5 ± 0.5
	19	WW-BS2-4	Ac-PLPPG-WEIRI-GSGSGS-**ISFY**-NHNT-KTT-TWERPRL-NH_2	37.0 ± 1.0
4	20	WW-LP2-1	Ac-PLPPG-WEIRI-GSGSGS-IYYY-**NSGS**-KTT-TWERPRL-NH_2	42.5 ± 0.5
	21	WW-LP2-2	Ac-PLPPG-WEIRI-GSGSGS-IYYY-**NEGS**-KTT-TWERPRL-NH_2	36.5 ± 0.5
	22	WW-LP2-3	Ac-PLPPG-WEIRI-GSGSGS-IYYY-**NSNS**-KTT-TWERPRL-NH_2	49.0 ± 0.5
	23	WW-LP2-4	Ac-PLPPG-WEIRI-GSGSGS-IYYY-**NSNT**-KTT-TWERPRL-NH_2	57.0 ± 0.5
	24	WW-LP2-5*	Ac-PLPPG-WEIRI-GSGSGS-IYYY-**NSIT**-KTT-TWERPRL-NH_2	64.5 ± 0.5
	25	WW-LP2-6	Ac-PLPPG-WEIRI-GSGSGS-IYYY-**NSLT**-KTT-TWERPRL-NH_2	63.5 ± 0.5
	26	WW-LP2-7	Ac-PLPPG-WEIRI-GSGSGS-IYYY-**NGSG**-KTT-TWERPRL-NH_2	< 0
	27	WW-LP2-8	Ac-PLPPG-WEIRI-GSGSGS-IYYY-**NGNG**-KTT-TWERPRL-NH_2	3.0 ± 5.0
	28	WW-LP2-9	Ac-PLPPG-WEIRI-GSGSGS-IYYY-**NGIT**-KTT-TWERPRL-NH_2	54.0 ± 0.5
5	29	WW-BS3-1	Ac-PLPPG-WEIRI-GSGSGS-IYYY-NSIT-**KTS**-TWERPRL-NH_2	63.0 ± 0.5
	30	WW-BS3-2	Ac-PLPPG-WEIRI-GSGSGS-IYYY-NSIT-**KTN**-TWERPRL-NH_2	50.5 ± 0.5
	31	WW-BS3-3	Ac-PLPPG-WEIRI-GSGSGS-IYYY-NSIT-**KTA**-TWERPRL-NH_2	64.0 ± 0.5
	32	WW-BS3-4	Ac-PLPPG-WEIRI-GSGSGS-IYYY-NSIT-**RTT**-TWERPRL-NH_2	62.5 ± 0.5
	33	WW-BS3-5	Ac-PLPPG-WEIRI-GSGSGS-IYYY-NSIT-**RTS**-TWERPRL-NH_2	61.5 ± 0.5
	34	WW-BS3-6	Ac-PLPPG-WEIRI-GSGSGS-IYYY-NSIT-**RTA**-TWERPRL-NH_2	62.5 ± 0.5
	35	WW-BS3-7[a]	Ac-PLPPG-WEIRI-GSGSGS-IYYY-NSIT-**RIT**-TWERPRL-NH_2	48.5 ± 0.5
6	36	WW-CT-1	Ac-PLPPG-WEIRI-GSGSGS-IYYY-NSIT-KTT-**TAERPRL**-NH_2	61.5 ± 0.5
	37	WW-CT-2	Ac-PLPPG-WEIRI-GSGSGS-IYYY-NSIT-KTT-**TWQRPRL**-NH_2	63.0 ± 0.5
	38	WW-CT-3	Ac-PLPPG-WEIRI-GSGSGS-IYYY-NSIT-KTT-**TWERP** -NH_2	63.5 ± 0.5

[a]Peptide aggregates over time; sequences highlighted in gray were taken to the next round of iterations. *Sequence taken to the two next rounds of iterations.

acids (WW-CT-3) also resulted in a well-folded and thermally stable WW-domain scaffold (Table 1, entry 38 and Figures S1f and S2f).

Sequence–Structure Relationship in a Thermally Stable WW Domain. In summary, the rounds of sequence iterations in WW-CS have shown that the WW-domain

scaffold is generally tolerant to a wide range of sequence variations. Based on these results, our goal was to design a highly thermostable core scaffold that could subsequently be used to design stably folded WW domain-based miniproteins with tailored functions. Structure-stabilizing sequence features were therefore the focus of our efforts. The following sequence features lead to a high degree of structure stabilization: (i) extension of the hydrophobic core in BS1 and LP2, (ii) presence of tyrosine at position 19 in BS2, (iii) existence of charges in BS1 (positions 7 and 9) and LP1 (positions 11 and 16).

A schematic representation of the sequence−structure relationship that should give a highly thermostable scaffold is shown in Figure 3a. Highly conserved residues that do not

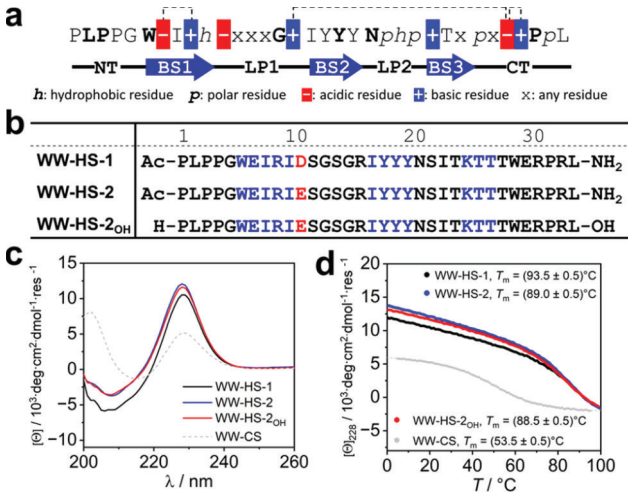

Figure 3. *De novo* designed highly thermostable WW-domain peptides. (a) Sequence−structure relationship in WW domains. Residues shown in bold are essential for structural integrity, and dotted lines indicate electrostatic interactions that were identified by NMR spectroscopy (*vide infra*). (b) Primary sequences of highly thermostable WW-domain peptides. β-Sheet regions are depicted in blue, disordered regions and loop regions in black. Sequences of WW-HS-1 and WW-HS-2 only vary in position 11 (red). (c) CD spectra acquired at 20 °C and (d) thermal denaturation profiles monitored at a wavelength of 228 nm of WW-HS-1, WW-HS-2, and WW-HS-2_{OH}. WW-CS CD data is shown as a reference (0.1 mM peptide, PBS, pH 7.5). CD spectra and thermal denaturation profiles are mean of triplicates.

tolerate modification are presented in bold. In addition, required charged residues are highlighted. Overall, amino acid residues that face the surface of the WW-domain scaffold or are part of LP1 are highly tolerant to sequence variations. This indicates that functionalization of the surface, which usually involves variation of several sequence positions while maintaining structural integrity, should indeed be possible.

Hyperthermostable WW-Domain Core Scaffold. The iterative modification of WW-CS allowed us to identify sequence features of the WW domain that are particularly structure-stabilizing. To design a highly thermostable WW-domain peptide that can serve as a core scaffold to be functionalized with receptor or catalytic properties (Figure 1c), we combined the most structurally stabilizing sequence motifs of the studied structure segments into one WW domain, which we refer to as WW-HS-1 (HS—highly stable). However, WW-HS-1 contains an aspartate in LP1 that might be prone to aspartimide formation (Figure 3b).[16] Hence, we also studied a variant with a glutamate at that position (WW-HS-2) and, additionally, the influence of charges at both termini with uncapped WW-HS-2_{OH} (Figure 3b).

WW-HS-2 and WW-HS-2_{OH} were synthesized using standard microwave-assisted solid-phase peptide synthesis. However, WW-HS-1 required a slightly different synthesis protocol to suppress aspartimide formation. We used the CSY protecting group invented by the Bode group on the side chain of the aspartate residue in question under the conditions recently optimized for the synthesis of β-sheet peptides.[17] We analyzed the structure and thermal stability of the WW-HS peptides by CD spectroscopy (Figure 3c,d). All peptides showed the characteristic CD spectrum with the pronounced exciton coupling at 228 nm. Thermal denaturation profiles revealed high thermal stabilities for WW-HS-1 and WW-HS-2 with melting temperatures of 93.5 and 89.0 °C, respectively. This is indeed remarkable since, to our knowledge, only one engineered WW domain with a similar degree of thermal stability has been reported, namely, WW st34, which displayed a melting temperature of 94 °C and was stabilized by tryptophan cross-strand interactions.[7c] WW-HS-2_{OH}, the uncapped variant of WW-HS-2, displayed a similar melting temperature of 88.5 °C, indicating that the charged termini located in close proximity do not provide additional structural stabilization through electrostatic interactions.

We also tested the reversibility of thermal unfolding but found when recording the cooling profiles that thermal unfolding was not fully reversible in any of the thermally stable variants (Figure S4). Considering that this might be due to the expansion of the hydrophobic core, particularly in BS1, we undertook a redesign of this sequence segment and introduced charged or polar residues (WW-HS-3 to WW-HS-5, Table S2 and Figure S5). These peptides were less thermally stable and also did not display reversible thermal denaturation. We therefore did not consider the second generation of WW-HS for further studies, especially since the first-generation peptides (WW-HS-1 and WW-HS-2) proved to be stable for several weeks in solution at room temperature (*vide infra*).

***De Novo* Designed Highly Thermostable Peptide Possesses WW-Domain Structure.** Multidimensional high-resolution NMR spectroscopy was used to determine the three-dimensional structure of WW-HS-2_{OH} at atomic resolution based on an almost complete assignment of two-dimensional heteronuclear $^{1}H-^{15}N$ as well as $^{1}H-^{13}C$ HSQC NMR spectra (Figures S6−S8). The structure determination was based on 424 NOEs (among them 153 classified as long-range) obtained from a two-dimensional $^{1}H-^{1}H$ NOESY spectrum and additional 27 dihedral angles obtained by running TALOS-N software[18] leading to a high convergence among the ten conformers that possess the lowest overall energy (Figure S6 and Table S3). Especially the orientation of side chains of residues W6 and Y19—both contributing to the hydrophobic core of the WW domain (Figure 2b)—are well conserved in analyzing the structural bundle (Figure 4b). Using the three-dimensional structure of WW-HS-2_{OH}, we assessed if it provides a rationale to understand the pronounced thermal stability. To answer this question, we have also made use of both AlphaFold2[19] and OmegaFold[20] packages to predict the three-dimensional structures of corresponding WW-HS-2_{OH}. The structure predictions resemble the backbone of the WW domain that has been experimentally determined by NMR spectroscopy to a high

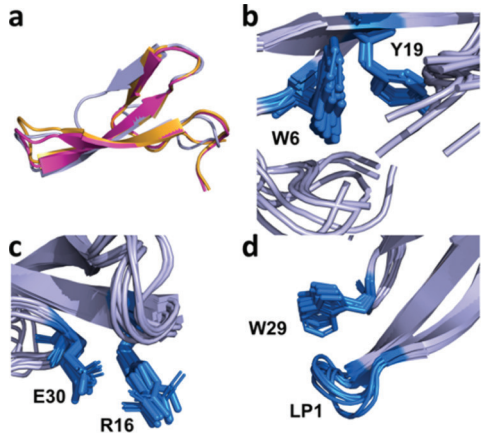

Figure 4. Three-dimensional structure determination of WW-HS-2_{OH}. (a) Structural alignment between the conformer of WW-HS-2_{OH} obtained from NMR spectroscopic data that possesses the lowest overall energy (colored in light blue) and structural characteristics of WW-HS-2_{OH} predicted by AlphaFold2 (colored in orange) and OmegaFold (colored in pink).[19,20] (b–d) Structural basis of WW-HS-2_{OH} illuminates structural features that may give rise to pronounced thermal stability observed for WW-HS-2_{OH} while aligning the five conformers possessing lowest overall energy. Close spatial contact between W6 and Y19 (b), formation of a salt bridge between R16 and E30 (c), and distinct hydrophobic contact between W29 and residues comprising LP1 (d) are highlighted. Orientation of side chain atoms is highlighted in blue.

degree (Figure 4a). Thus, the lengths of BS1, BS2, and BS3 are the same, and LP1 and LP2 are formed in a comparable manner. However, the position of BS3 differs in the direction to CT when experimentally determined and predicted structures are compared. In consequence, BS2 and BS3 are placed coplanar in the experimentally determined structure in contrast to the predicted structures in which BS2 and BS3 are rather twisted with each other.

Focusing on residues W6 and Y19 comprising the hydrophobic core (*vide supra*) shows a high similarity in the orientation of corresponding side chains when the structural bundle of WW-HS-2_{OH} is analyzed. The close distance among them may explain the pronounced exciton coupling observed for WW-HS-2_{OH} (Figures 3c and 4b). In addition, the incorporation of isoleucine residues, particularly in BS1, led to an expansion of the hydrophobic core, as anticipated. Another potential reason for the pronounced thermal stability of WW-HS-2_{OH} lies in the presence of a prominent salt bridge formed between R16 and E30 (Figure 4c). This important long-range interaction has also been added as an additional structure–function relationship to the scheme shown in Figure 3a. Third, the orientation of the side chain of W29 in WW-HS-2_{OH} facilitates prominent local contacts to residues comprising LP1 (Figure 4d). This close proximity between hydrophobic W29 and LP1 may also contribute to the significant stabilization of WW-HS-2_{OH} leading then to the increased thermal stability that is observed. Indeed, when we iterated the CT sequence, we found that replacing W29 with alanine resulted in a decrease in T_m of 3 K.

To conclude the structural studies, and out of curiosity, we applied ProteinMPNN[21] to the NMR structure to compare proposed sequences with experimental results. At first glance, sequence patterns proposed by ProteinMPNN appeared different from the experimentally determined sequence–structure relationship (Figure S9). The amino acid compositions of NT, BS1, BS3, and CT differ, and the NMR-determined long-range interaction between sequence positions R16 and E30 was not predicted. However, conserved sequence positions such as Gly15, N21, and the hydrophobic core as well as the pronounced aromatic content found for BS2 are predicted in agreement with the experimental findings.

WW-HS-2 Serves as a Core Scaffold for the Design of Functional WW Domains. A highly thermostable scaffold like WW-HS-2 should be suitable to be engineered into a functional miniprotein (Figure 1d). To test this hypothesis, we aimed to engineer the molecular recognition of the binding motifs of the three WW-domain groups on WW-HS-2. WW domains of Group I bind proline-rich motifs of the type PPxY (x: any amino acid), ligands of Group II/III show a characteristic PPLP/PPRP motif, and those of Group IV bind phosphorylated ligands of the type pS/pTP.[22] Using computer-simulated alanine scanning on existing NMR spectroscopic and X-ray crystal structures solved for WW domains of the respective groups, we were able to identify residues at the ligand-binding sites that are important for the function of the respective WW domain (Table S4).[23] We then grafted these relevant sequence features onto the surface of WW-HS-2. The resulting sequences for the designed WW-domain representatives of each group are shown in Figure 5a,b.

The corresponding WW domains were synthesized and first analyzed for structure and thermal stability. The three *de novo* designed peptides showed the characteristic signature in their respective CD spectra with the intense exciton signal at 228 nm (Figure 5c). The thermal stabilities of the three peptides determined by CD spectroscopy were lower than that of WW-HS-2 but still possessed melting temperatures above 75 °C that can be rated as high (Figure 5d). This is remarkable because, in WW-HS-2, up to six residues were changed to create the desired function. This confirms the initial hypothesis that when a highly thermostable WW-domain scaffold is utilized for functionalization, the resulting scaffold should still possess good thermal stability. Just aside, we also synthesized three native WW domains, one representative of each group, which all displayed significantly lower thermal stabilities than the designed equivalents (Figure S10).

Finally, we determined the binding affinities of the three designed WW domains to corresponding group-specific ligands (see Figure 5e for sequences) by monitoring the changes in intrinsic fluorescence of tryptophan residues upon ligand titration. We then determined the binding dissociation constants (K_d values) from the resulting saturation binding curves and compared them with the K_d values of the reference WW domains yYAP1_{WW2} (Group I), hGas7_{WW} (Group II/III), and hPin1_{WW} (Group IV) (Figure S9d,e). All three designed WW domains bind corresponding ligands with K_d values in the low micromolar range and comparable to the chosen references (Figures 5e and S10). Only the reference peptide yYap1_{WW2} showed moderate binding to ligand Group I, which was 2 orders of magnitude higher than that of WW-HS-I but in agreement with the literature (Figure S10).[25] We would like to emphasize that we did not optimize the binding properties but simply grafted the binding-relevant residues identified by computer simulation to our experimentally determined highly thermostable WW-domain core scaffold WW-HS-2, as described above. These three examples thus demonstrate that (a) WW-HS-2 behaves robustly to engineering and (b) WW-

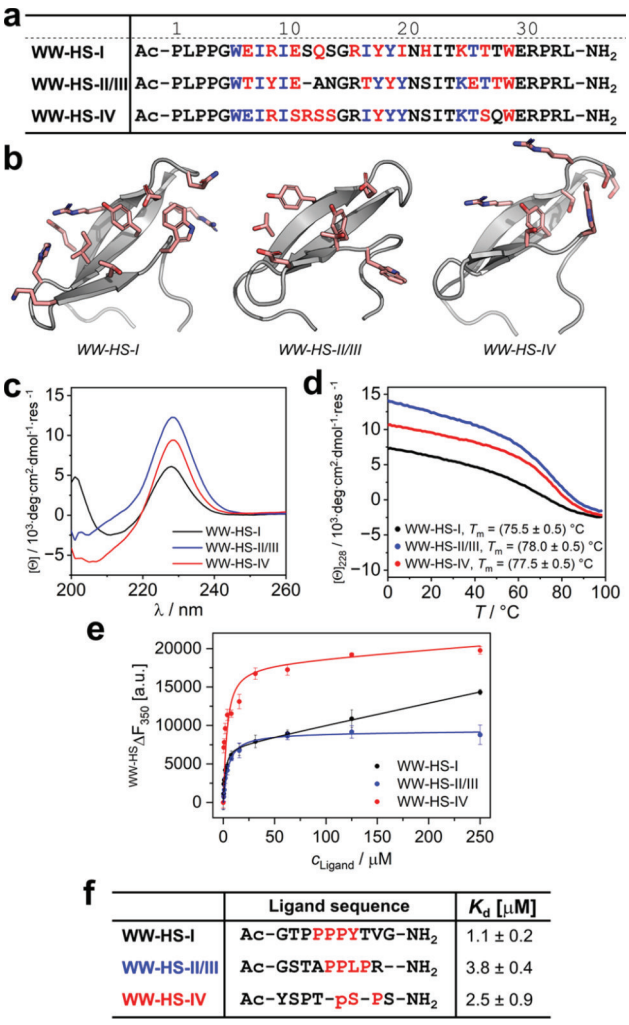

Figure 5. *De novo* designed thermostable functional WW domains. (a) Sequences of thermostable WW domains with binding properties of Group I (WW-HS-I), Group II/III (WW-HS-II/III), and Group IV (WW-HS-IV). Residues shown in blue indicate β-sheet regions. (b) Computational structural models of WW-HS-I, WW-HS-II/III, and WW-HS-IV generated from the high-resolution NMR structure of WW-HS-2_{OH} and the relax function of the Rosetta software package.[24] Residues involved in ligand binding are displayed in pink. (c) CD spectra at 20 °C and (d) thermal denaturation monitored at 228 nm of functional thermostable *de novo* designed WW domains WW-HS-I, WW- HS-II/III, and WW-HS-IV (0.1 mM peptide, PBS, pH 7.5). CD spectra and thermal denaturation profiles are mean of triplicates. (e) Intrinsic tryptophan fluorescence titrations of WW-domain group-specific ligands to determine K_d values of WW-HS-I, WW-HS-II/III, and WW-HS-IV. (f) Sequences of WW-domain group-specific ligands and corresponding K_d values obtained from nonlinear least-squares fitting to the saturation binding curves (see SI eq 4; 2 μM peptide, PBS, pH 7.5, room temperature, 0−250 μM peptide ligand).

HS-2 can be functionalized by grafting arbitrary binding motifs on its surface while maintaining a high thermostability.

Design of Stably Folded WW-Domain Minireceptors. Encouraged by the success in designing thermostable *de novo* WW domains, we decided to go one step further and design WW domains with non-native functions using WW-HS-1 as a starting point. By top-down engineering of the natural WW domain hPin1_{WW}, minireceptors with metal ion and even organophosphate-binding properties have already been generated.[7d,8b] However, these WW domain-based functional peptides showed, at best, moderate thermal stability. We hypothesized that grafting the potential binding motifs onto the highly thermostable WW domain should yield functional WW-domain minireceptors with good thermal stability.

First, we designed a thermostable metal-binding miniprotein. Previously, we had obtained a Zn(II)-binding WW domain by grafting a His_3 metal-binding site onto the surface of hPin1_{WW}.[8b] The resulting peptide, WW-CA, was a molten globule in the apo state but was able to partially restore the structure of the WW domain upon binding of Zn(II) *via* the His_3 site displaying a moderate thermal stability, with a melting temperature of 34 °C. Two rounds of sequence redesign, *e.g.*, engineering of LP1, were then required to obtain a thermostable WW-domain-Zn(II) complex, WW-CA-ANG-Zn(II), with a melting temperature of 70 °C.[8d] We anticipated that grafting the His_3 site onto WW-HS-1 would provide a thermostable Zn(II)-binding WW domain in one step without the need for further sequence redesign. We synthesized WW-HS-CA (Figure 6a,b) and investigated its structure and thermostability, as well as its Zn(II)-binding properties.

The CD spectrum of the apo peptide is characteristic of a WW domain (Figure 6c). Upon addition of Zn(II), the intensity of the exciton signal at 228 nm decreased, indicating conformational changes due to Zn(II) binding. Thermal CD denaturation experiments showed cooperative folding-to-unfolding of the apo- and holo-peptide and T_m values of 43 and 75.5 °C, respectively (Figure 6d). Thus, WW-HS-CA-Zn(II) can be considered thermostable. Furthermore, the measured T_m values for the apo peptide and the Zn(II) complex are higher than those for WW-CA-ANG. Finally, we performed competitive titration experiments with MagFura2 as competitor to study Zn(II) binding to WW-HS-CA and determined a K_d value of 0.1 μM, which is five times lower than that of WW-CA-ANG and Zn(II) and more than 10 times lower than that of WW-CA (Figure 6e). Thus, not only did we improve the thermostability, but we also obtained a metallo-minireceptor with further improved function.

To increase the complexity, we engineered the binding of organophosphates to WW-HS-1. The adenosine triphosphate (ATP)- and phosphocholine (PC)-binding WW domains, WW-2−10-ATP and WW-1−8-PC, were recently identified by combinatorial screening on split variants of hPin1_{WW}.[7d] The two WW domains bind their respective ligands with K_d values in the micromolar range (14 μM (WW-2−10-ATP) and 1.1 μM (WW-1−8-PC)). However, WW-2−10-ATP was moderately thermostable, with a T_m value of 36 °C, while WW-1−8-PC was only partially folded at 20 °C (T_m = 14 °C). We identified the amino acid residues important for the respective ligand binding by computational modeling with AlphaFold2 and subsequent docking with AutoDock Vina[26] (Figure S11) and grafted the binding motifs onto WW-HS-1, yielding the WW-domain variants WW-HS-ATP and WW-HS-PC (Figure 6a,b). After chemical synthesis, both peptides were characterized with respect to their structure and thermal stability. CD spectra indicated a well-folded WW-domain scaffold in both cases (Figure 6f). Thermal denaturation experiments revealed cooperative folding-to-unfolding and T_m values of 58 °C for WW-HS-ATP and 47.5 °C for WW-HS-PC (Figure 6g). In the case of WW-HS-PC, this is an increase of 34 K compared to WW-1−8-PC obtained by top-down engineering of hPin1_{WW}. Binding to the respective organophosphates was then investigated by monitoring tryptophan

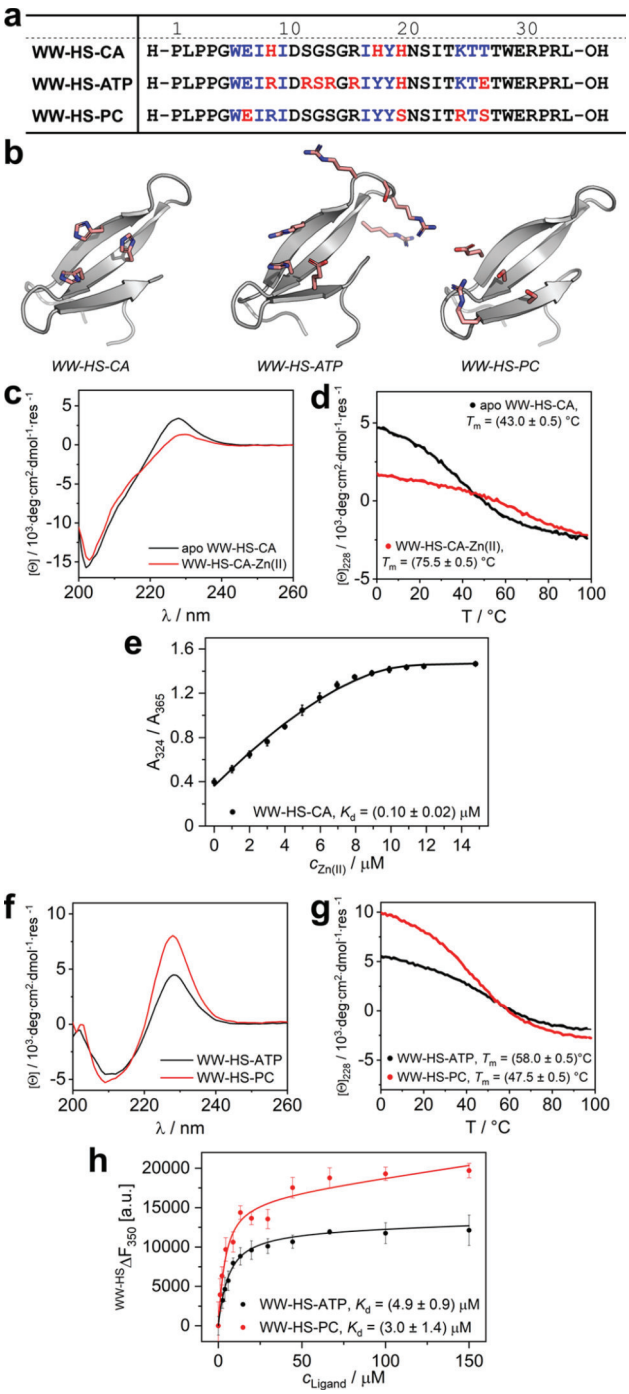

Figure 6. *De novo* designed WW-domain minireceptors. (a) Sequences of WW-domain minireceptors with Zn(II), ATP, and PC binding properties. Residues shown in blue indicate β-sheet regions, and residues depicted in red indicate binding motifs. (b) Computational structural models of WW-HS-CA, WW-HS-ATP, and WW-HS-PC generated from the high-resolution NMR structure of WW-HS-2_{OH} and the relax function of the Rosetta software package.[24] Residues involved in ligand binding are displayed in pink. (c) CD spectra at 20 °C and (d) thermal denaturation profiles monitored at 228 nm of WW-HS-CA in the apo and holo state (0.1 mM peptide, 0.1 mM $ZnSO_4$ (if present), MOPS-buffered saline, pH 7.2). CD spectra and thermal denaturation profiles are mean of duplicates. (e) Competitive titration experiments of WW-HS-CA with Zn(II) in the presence of MagFura2 (5 μM peptide, 5 μM MagFura2, MOPS-buffered saline, pH 7.2 titrated with 1 mM $ZnSO_4$ in MOPS-buffered saline). The error bars display the standard deviation of three independent measurements (for details, see the SI). (f) CD spectra at 20 °C and (g) thermal denaturation profiles monitored at 228 nm of WW-HS-ATP and WW-HS-PC (0.1 mM peptide, PBS, pH 7.5). CD spectra and thermal denaturation profiles are mean of duplicates. (h) Intrinsic tryptophan fluorescence titrations of ATP or PC to WW-HS-ATP (black) or WW-HS-PC (red). The corresponding K_d values were determined from nonlinear least-squares fitting to the saturation binding curves (see SI eq 4; 2 μM (WW-HS-ATP) or 1 μM peptide (WW-HS-PC), PBS, pH 7.5, room temperature; 0−150 μM ligand).

fluorescence quenching in the WW-domain minireceptors upon ligand titration (Figure 6h). Numerical values for K_d were determined by nonlinear least-squares fitting to the resulting saturation binding curves and were in the low micromolar range for both minireceptors and their respective ligands. This is in the same regime as the K_d values of the $hPin1_{WW}$-derived minireceptors, which are 14 μM for ATP binding to WW-2−10-ATP and 1.1 μM for PC binding to WW-1−8-PC.[7d]

CONCLUSIONS

In this report, we presented the design of highly thermostable WW domains WW-HS-1 and WW-HS-2 to be used as core scaffolds to create stably folded functional WW-domain miniproteins on demand in a top-down engineering approach. Sequence−structure relationships were identified through several rounds of iterative variations of a consensus sequence WW-CS that was directed from the N- to the C-terminus and allowed us to identify structure-stabilizing sequence features. Based on these results, we designed two hyperthermostable WW-domain scaffolds, WW-HS-1 and WW-HS-2, which displayed melting temperatures of 93.5 and 89 °C, respectively. Using multidimensional NMR spectroscopy, the highly resolved three-dimensional structure of WW-HS-2_{OH}, the uncapped variant of WW-HS-2, was obtained. Tight packing of the hydrophobic core, a long-range salt bridge between R16 and E30 and hydrophobic contacts between LP1 and W29 are characteristic structural features that may explain the high thermal stability found for WW-HS-2_{OH}. To prove the suitability of the highly thermostable WW domains to act as core scaffolds for the design of functional WW-domain miniproteins, we first grafted the binding motifs of Group I, Group II/III, and Group IV WW domains onto the surface of WW-HS-2 and obtained highly thermostable *de novo* WW domains that indeed displayed the three different binding modes that were intended. The customizability of the thermostable scaffolds was demonstrated by designing stably folded WW domain-like minireceptors with organophosphate and metal ion binding properties by grafting the respective binding motifs onto the surface of WW-HS-1.

The field of miniprotein research has been dominated by α-helical scaffolds, in particular, the coiled coil.[1,27] There are also β-sheet scaffolds that have shown potential for the development of diagnostic tools and therapeutics, such as affimers and nanobodies,[28] but due to their molecular size, they cannot be considered as miniproteins. The only β-sheet miniprotein scaffolds whose potential for medical applications has been recognized to date are the cyclotides, cyclic peptides with a cysteine knot motif that are very stable and resistant to proteolytic degradation.[29] However, because of their cyclic and

knotted structure, chemical synthesis is not straightforward. Small linear β-sheet peptides have, to some degree, been studied but never brought to applications.[6f] This includes the WW domains that have rarely been used to develop functional building blocks for synthetic biology or biomaterial design applications.[8a−c] One reason for this lack of use may be the absence of a basis set of well-described, reliably and stably folding β-sheet scaffolds that can be easily modified for an intended application. Such basis sets exist, e.g., for coiled-coil motifs that have been readily used as tool sets by scientists working in the afore research areas.[29] Although WW domains have been used as model systems to study various aspects of protein folding,[6a,7b,9a,b,30] to our knowledge, these studies have not led to the design of a core scaffold that can be used to design stably folded functional miniproteins. With the design of the highly thermostable WW-HS scaffolds, we provide the first robustly folded WW domains that can be used as platforms for the on-demand design of functional β-sheet miniproteins. The WW-HS scaffolds not only exhibit excellent thermostability—indeed, they can be considered hyperthermostable—but they also exhibit excellent threshold robustness, providing even well-folded WW domain-like scaffolds with good thermostabilities after highly destabilizing sequence variations, such as the incorporation of polar or charged residues into the highly conserved BS2. Here, we have presented the design of well-folded and stable WW-HS-derived WW-domain miniproteins with peptide, metal ion and organophosphate recognition (Figure 1). However, we believe that WW-HS will be the source for the design of a truly broad range of functional β-sheet miniproteins with receptive, sensory, and even catalytic properties.

■ ASSOCIATED CONTENT

● Supporting Information

The Supporting Information is available free of charge at https://pubs.acs.org/doi/10.1021/jacs.4c03498.

> Experimental procedures; sequences and melting temperatures of highly stable WW domains WW-HS-3, WW-HS-4, WW-HS-5; NMR statistics analyzing ten conformers possessing lowest overall energy; thermal unfolding and refolding studies on WW-HS-1 and WW-HS-2; sequence prediction; full characterization of the peptides investigated (PDF)

Accession Codes

Values of chemical shifts obtained by multidimensional high-resolution NMR spectroscopy have been deposited into the BMRB using the accession number 52114; the structural bundle of WW-HS-2 possessing the lowest overall energy has been uploaded into the PDB (entry ID 8QTQ).

■ AUTHOR INFORMATION

Corresponding Authors

Michael Kovermann − *Physical Chemistry, University of Konstanz, 78457 Konstanz, Germany;* orcid.org/0000-0002-3357-9843; Email: michael.kovermann@uni-konstanz.de

Franziska Thomas − *Institute of Organic Chemistry, Heidelberg University, 69120 Heidelberg, Germany;* orcid.org/0000-0002-1176-7018; Email: franziska.thomas@oci.uni-heidelberg.de

Authors

Christina Lindner − *Institute of Organic Chemistry, Heidelberg University, 69120 Heidelberg, Germany*

Anke Friemel − *Physical Chemistry, University of Konstanz, 78457 Konstanz, Germany*

Niklas Schwegler − *Institute of Organic Chemistry, Heidelberg University, 69120 Heidelberg, Germany; Institute for Molecular Systems Engineering and Advanced Materials, Heidelberg University, 69120 Heidelberg, Germany;* orcid.org/0000-0002-0954-7956

Lisa Timmermann − *Institute of Organic Chemistry, Heidelberg University, 69120 Heidelberg, Germany*

Truc Lam Pham − *Institute of Organic Chemistry, Heidelberg University, 69120 Heidelberg, Germany;* orcid.org/0000-0003-3808-2083

Vanessa Reusche − *Institute of Organic Chemistry, Heidelberg University, 69120 Heidelberg, Germany*

Complete contact information is available at: https://pubs.acs.org/10.1021/jacs.4c03498

Author Contributions

The manuscript was written through contributions of all authors.

Funding

This work was supported by the Deutsche Forschungsgemeinschaft (DFG, German Research Foundation) 414261058 and by the DFG under Germany's Excellence Strategy 2082/1 390761711. N.S. is grateful to the Evangelisches Studienwerk Villigst e.V. for support through a Doctoral Scholarship and to the Joachim Herz Foundation for support through the Add-On Fellowship for Interdisciplinary Life Sciences. T.L.P. was supported by the Fonds der Chemischen Industrie through a Kekulé Fellowship. M.K. acknowledges the permanent financial support for the NMR core facility provided by the University of Konstanz. This study was conducted within the Max Planck School Matter to Life, supported by the German Federal Ministry of Education and Research (BMBF), in collaboration with the Max Planck Society.

Notes

The authors declare no competing financial interest.

■ ACKNOWLEDGMENTS

The authors are grateful to Prof. Dr. Christian Klein (Heidelberg University) for providing access to a CD spectrometer. The authors thank Frederic Berner for supporting the upload of experimental data into BMRB and PDB and Marcos Conde González for performing the ProteinMPNN prediction.

■ REFERENCES

(1) Baker, E. G.; Bartlett, G. J.; Goff, K. L. P.; Woolfson, D. N. Miniprotein Design: Past, Present, and Prospects. *Acc. Chem. Res.* **2017**, *50* (9), 2085−2092.

(2) (a) Crook, Z. R.; Nairn, N. W.; Olson, J. M. Miniproteins as a Powerful Modality in Drug Development. *Trends Biochem. Sci.* **2020**, *45* (4), 332−346. (b) Ożga, K.; Berlicki, Ł. Design and Engineering of Miniproteins. *ACS Bio Med Chem Au* **2022**, *2* (4), 316−327.

(3) Teufl, M.; Zajc, C. U.; Traxlmayr, M. W. Engineering Strategies to Overcome the Stability−Function Trade-Off in Proteins. *ACS Synth. Biol.* **2022**, *11* (3), 1030−1039.

(4) (a) Greaves, R. B.; Warwicker, J. Mechanisms for stabilisation and the maintenance of solubility in proteins from thermophiles. *BMC Struct. Biol.* **2007**, *7* (1), No. 18. (b) Rothschild, L. J.; Mancinelli, R.

L. Life in extreme environments. *Nature* **2001**, *409* (6823), 1092−1101.
(5) Blanchard, P. L.; Knick, B. J.; Whelan, S. A.; Hackel, B. J. Hyperstable Synthetic Mini-Proteins as Effective Ligand Scaffolds. *ACS Synth. Biol.* **2023**, *12* (12), 3608−3622.
(6) (a) Jäger, M.; Dendle, M.; Kelly, J. W. Sequence determinants of thermodynamic stability in a WW domain—An all-β-sheet protein. *Protein Sci.* **2009**, *18* (8), 1806−1813. (b) Pires, J. R.; Taha-Nejad, F.; Toepert, F.; Ast, T.; Hoffmüller, U.; Schneider-Mergener, J.; Kühne, R.; Macias, M. J.; Oschkinat, H. Solution structures of the YAP65 WW domain and the variant L30 K in complex with the peptides GTPPPPYTVG, N-(n-octyl)-GPPPY and PLPPY and the application of peptide libraries reveal a minimal binding epitope. *J. Mol. Biol.* **2001**, *314* (5), 1147−1156. (c) Macias, M. J.; Hyvönen, M.; Baraldi, E.; Schultz, J.; Sudol, M.; Saraste, M.; Oschkinat, H. Structure of the WW domain of a kinase-associated protein complexed with a proline-rich peptide. *Nature* **1996**, *382* (6592), 646−649. (d) Tian, P.; Best, R. B. How Many Protein Sequences Fold to a Given Structure? A Coevolutionary Analysis. *Biophys. J.* **2017**, *113* (8), 1719−1730. (e) Fernández-Escamilla, A. M.; Ventura, S.; Serrano, L.; Jiménez, M. A. Design and NMR conformational study of a β-sheet peptide based on Betanova and WW domains. *Protein Sci.* **2006**, *15* (10), 2278−2289. (f) Thomas, F.; Pham, T. L. Design of Functional Globular β-Sheet Miniproteins. *ChemBioChem* **2024**, *25*, No. e202300745.
(7) (a) Anderson, J. M.; Andersen, N. H. A pH Switch for β-Sheet Protein Folding. *Angew. Chem., Int. Ed.* **2017**, *56* (25), 7074−7077. (b) Jäger, M.; Zhang, Y.; Bieschke, J.; Nguyen, H.; Dendle, M.; Bowman, M. E.; Noel, J. P.; Gruebele, M.; Kelly, J. W. Structure−function−folding relationship in a WW domain. *Proc. Natl. Acad. Sci. U.S.A.* **2006**, *103* (28), 10648−10653. (c) Kier, B. L.; Anderson, J. M.; Andersen, N. H. Circular Permutation of a WW Domain: Folding Still Occurs after Excising the Turn of the Folding-Nucleating Hairpin. *J. Am. Chem. Soc.* **2014**, *136* (2), 741−749. (d) Neitz, H.; Paul, N. B.; Häge, F. R.; Lindner, C.; Graebner, R.; Kovermann, M.; Thomas, F. Identification of novel functional mini-receptors by combinatorial screening of split-WW domains. *Chem. Sci.* **2022**, *13* (31), 9079−9090.
(8) (a) Stewart, A. L.; Park, J. H.; Waters, M. L. Redesign of a WW Domain Peptide for Selective Recognition of Single-Stranded DNA. *Biochemistry* **2011**, *50* (13), 2575−2584. (b) Pham, T. L.; Kovermann, M.; Thomas, F. Switchable Zinc(II)-Responsive Globular β-Sheet Peptide. *ACS Synth. Biol.* **2022**, *11* (1), 254−264. (c) Werner, M.; Pampel, J.; Pham, T. L.; Thomas, F. Late-Stage Functionalisation of Peptides on the Solid Phase by an Iodination-Substitution Approach. *Chem. - Eur. J.* **2022**, *28* (50), No. e202201339. (d) Pham, T. L.; González, M. R. C.; Fazliev, S.; Kishore, A.; Comba, P.; Thomas, F. Relationship of Thermostability and Binding Affinity in Metal-binding WW-Domain Minireceptors. *ChemBioChem* **2024**, *25*, No. e202300715.
(9) (a) Russ, W. P.; Lowery, D. M.; Mishra, P.; Yaffe, M. B.; Ranganathan, R. Natural-like function in artificial WW domains. *Nature* **2005**, *437* (7058), 579−583. (b) Socolich, M.; Lockless, S. W.; Russ, W. P.; Lee, H.; Gardner, K. H.; Ranganathan, R. Evolutionary information for specifying a protein fold. *Nature* **2005**, *437* (7058), 512−518. (c) Macias, M. J.; Gervais, V.; Civera, C.; Oschkinat, H. Structural analysis of WW domains and design of a WW prototype. *Nat. Struct. Biol.* **2000**, *7* (5), 375−379.
(10) Greenfield, N. J. Using circular dichroism collected as a function of temperature to determine the thermodynamics of protein unfolding and binding interactions. *Nat. Protoc.* **2006**, *1* (6), 2527−2535.
(11) Crooks, G. E.; Hon, G.; Chandonia, J.-M.; Brenner, S. E. WebLogo: a sequence logo generator. *Genome Res.* **2004**, *14* (6), 1188−1190.
(12) (a) Richardson, J. S.; Richardson, D. C. Natural β-sheet proteins use negative design to avoid edge-to-edge aggregation. *Proc. Natl. Acad. Sci. U.S.A.* **2002**, *99* (5), 2754−2759. (b) Minor, D. L.; Kim, P. S. Measurement of the β-sheet-forming propensities of amino acids. *Nature* **1994**, *367* (6464), 660−663.
(13) Chichili, V. P. R.; Kumar, V.; Sivaraman, J. Linkers in the structural biology of protein−protein interactions. *Protein Sci.* **2013**, *22* (2), 153−167.
(14) Shaw, D. E.; Maragakis, P.; Lindorff-Larsen, K.; Piana, S.; Dror, R. O.; Eastwood, M. P.; Bank, J. A.; Jumper, J. M.; Salmon, J. K.; Shan, Y.; Wriggers, W. Atomic-level characterization of the structural dynamics of proteins. *Science* **2010**, *330* (6002), 341−346.
(15) (a) Kowalski, J. A.; Liu, K.; Kelly, J. W. NMR solution structure of the isolated Apo Pin1 WW domain: Comparison to the x-ray crystal structures of Pin1. *Biopolymers* **2002**, *63* (2), 111−121. (b) Shaw, A. Z.; Martin-Malpartida, P.; Morales, B.; Yraola, F.; Royo, M.; Macias, M. J. Phosphorylation of either Ser16 or Thr30 does not disrupt the structure of the Itch E3 ubiquitin ligase third WW domain. *Proteins: Struct., Funct., Genet.* **2005**, *60* (3), 558−560.
(16) Subirós-Funosas, R.; El-Faham, A.; Albericio, F. Aspartimide formation in peptide chemistry: occurrence, prevention strategies and the role of N-hydroxylamines. *Tetrahedron* **2011**, *67* (45), 8595−8606.
(17) (a) Neumann, K.; Farnung, J.; Baldauf, S.; Bode, J. W. Prevention of aspartimide formation during peptide synthesis using cyanosulfurylides as carboxylic acid-protecting groups. *Nat. Commun.* **2020**, *11* (1), No. 982. (b) Pham, T. L.; Zilke, J.; Müller, C. C.; Thomas, F. The CSY-protecting group in the microwave-assisted synthesis of aggregation-prone peptides. *RSC Chem. Biol.* **2022**, *3* (4), 426−430.
(18) Shen, Y.; Bax, A. Protein backbone and sidechain torsion angles predicted from NMR chemical shifts using artificial neural networks. *J. Biomol. NMR* **2013**, *56* (3), 227−241.
(19) Jumper, J.; Evans, R.; Pritzel, A.; Green, T.; Figurnov, M.; Ronneberger, O.; Tunyasuvunakool, K.; Bates, R.; Žídek, A.; Potapenko, A.; et al. Highly accurate protein structure prediction with AlphaFold. *Nature* **2021**, *596* (7873), 583−589.
(20) Wu, R.; Ding, F.; Wang, R.; Shen, R.; Zhang, X.; Luo, S.; Su, C.; Wu, Z.; Xie, Q.; Berger, B. et al. High-resolution *de novo* structure prediction from primary sequence *bioRxiv* 2022, DOI: 10.1101/2022.07.21.500999 (accessed July 22, 2022).
(21) Dauparas, J.; Anishchenko, I.; Bennett, N.; Bai, H.; Ragotte, R. J.; Milles, L. F.; Wicky, B. I. M.; Courbet, A.; de Haas, R. J.; Bethel, N.; et al. Robust deep learning−based protein sequence design using ProteinMPNN. *Science* **2022**, *378* (6615), 49−56.
(22) (a) Kato, Y.; Nagata, K.; Takahashi, M.; Lian, L.; Herrero, J. J.; Sudol, M.; Tanokura, M. Common mechanism of ligand recognition by group II/III WW domains: Redefining their functional classification. *J. Biol. Chem.* **2004**, *279* (30), 31833−31841. (b) Meiyappan, M.; Birrane, G.; Ladias, J. A. A. Structural Basis for Polyproline Recognition by the FE65 WW Domain. *J. Mol. Biol.* **2007**, *372* (4), 970−980. (c) Chen, F.; Wang, Q.; Mu, Y.; Sun, S.; Yuan, X.; Shang, P.; Ji, B. Systematic profiling and identification of the peptide-mediated interactions between human Yes-associated protein and its partners in esophageal cancer. *J. Mol. Recognit.* **2022**, *35* (3), No. e2947.
(23) Kortemme, T.; Kim, D. E.; Baker, D. Computational Alanine Scanning of Protein-Protein Interfaces. *Sci. STKE* **2004**, *2004* (219), No. pl2.
(24) (a) Nivón, L. G.; Moretti, R.; Baker, D. (2013) A Pareto-Optimal Refinement Method for Protein Design Scaffolds. *PLoS One* **2013**, *8* (4), No. e59004. (b) Conway, P.; Tyka, M. D.; DiMaio, F.; Konerding, D.; Baker, D. Relaxation of backbone bond geometry improves protein energy landscape modeling. *Protein Sci.* **2014**, *23*, 47−55. (c) Khatib, F.; Cooper, S.; Tyka, M. D.; Xu, K.; Makedon, I.; Popović, Z.; Baker, D.; Players, F. Algorithm discovery by protein folding game players. *Proc. Natl. Acad. Sci. U.S.A.* **2011**, *108* (47), 18949−18953. (d) Tyka, M. D.; Keedy, D. A.; André, I.; DiMaio, F.; Song, Y.; Richardson, D. C.; Richardson, J. S.; Baker, D. Alternate States of Proteins Revealed by Detailed Energy Landscape Mapping. *J. Mol. Biol.* **2011**, *405* (2), 607−618.
(25) Webb, C.; Upadhyay, A.; Giuntini, F.; Eggleston, I.; Furutani-Seiki, M.; Ishima, R.; Bagby, S. Structural features and ligand binding properties of tandem WW domains from YAP and TAZ, nuclear

effectors of the Hippo pathway. *Biochemistry* **2011**, *50* (16), 3300−3309.
(26) (a) Trott, O.; Olson, A. J. AutoDock Vina: Improving the speed and accuracy of docking with a new scoring function, efficient optimization, and multithreading. *J. Comput. Chem.* **2010**, *31* (2), 455−461. (b) Forli, S.; Huey, R.; Pique, M. E.; Sanner, M. F.; Goodsell, D. S.; Olson, A. J. Computational protein−ligand docking and virtual drug screening with the AutoDock suite. *Nat. Protoc.* **2016**, *11* (5), 905−919.
(27) (a) Fletcher, J. M.; Boyle, A. L.; Bruning, M.; Bartlett, G. J.; Vincent, T. L.; Zaccai, N. R.; Armstrong, C. T.; Bromley, E. H. C.; Booth, P. J.; Brady, R. L.; et al. A Basis Set of de Novo Coiled-Coil Peptide Oligomers for Rational Protein Design and Synthetic Biology. *ACS Synth. Biol.* **2012**, *1* (6), 240−250. (b) Groth, M. C.; Rink, W. M.; Meyer, N. F.; Thomas, F. Kinetic studies on strand displacement in de novo designed parallel heterodimeric coiled coils. *Chem. Sci.* **2018**, *9* (18), 4308−4316. (c) Rink, W. M.; Thomas, F. De Novo Designed α-Helical Coiled-Coil Peptides as Scaffolds for Chemical Reactions. *Chem. - Eur. J.* **2019**, *25* (7), 1665−1677. (d) Thomas, F. α-Helix and Coiled-Coil Peptide Nanomaterials. In *Peptide Bionanomaterials: From Design to Application*; Elsawy, M. A., Ed.; Springer International Publishing, 2023; pp 87−119.
(28) (a) Gebauer, M.; Skerra, A. Engineering of binding functions into proteins. *Curr. Opin. Biotechnol.* **2019**, *60*, 230−241. (b) Cordell, P.; Carrington, G.; Curd, A.; Parker, F.; Tomlinson, D.; Peckham, M. *J. Cell Sci.* **2022**, *135*, No. jcs259168. (c) Schumacher, D.; Helma, J.; Schneider, A. F. L.; Leonhardt, H.; Hackenberger, C. P. R. Nanobodies: Chemical Functionalization Strategies and Intracellular Applications. *Angew. Chem., Int. Ed.* **2018**, *57*, 2314−2333.
(29) de Veer, S. J.; Kan, M.-W.; Craik, D. J. Cyclotides: From Structure to Function. *Chem. Rev.* **2019**, *119*, 12375−12421.
(30) Jäger, M.; Deechongkit, S.; Koepf, E. K.; Nguyen, H.; Gao, J.; Powers, E. T.; Gruebele, M.; Kelly, J. W. Understanding the mechanism of β-sheet folding from a chemical and biological perspective. *Pept. Sci.* **2008**, *90* (6), 751−758.